# Accepted Manuscript

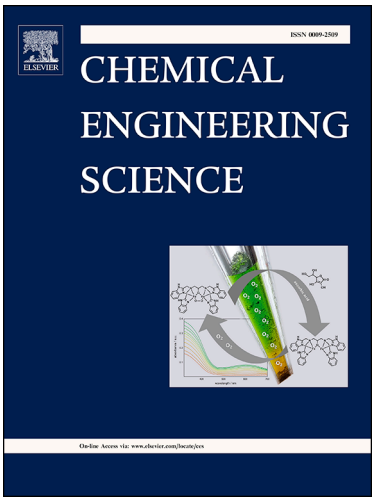


The distortion of a horizontal soap film due to the impact of a falling sphere

C.H. Chen, A. Perera, P. Jackson, B. Hallmark, J.F. Davidson

PII: S0009-2509(19)30413-0
DOI: https://doi.org/10.1016/j.ces.2019.04.041
Reference: CES 14952

To appear in: *Chemical Engineering Science*

Received Date: 1 February 2019
Revised Date: 23 April 2019
Accepted Date: 27 April 2019

Please cite this article as: C.H. Chen, A. Perera, P. Jackson, B. Hallmark, J.F. Davidson, The distortion of a horizontal soap film due to the impact of a falling sphere, *Chemical Engineering Science* (2019), doi: https://doi.org/10.1016/j.ces.2019.04.041

# The distortion of a horizontal soap film due to the impact of a falling sphere

**C.H. Chen, A. Perera, P. Jackson, B. Hallmark, J.F. Davidson**

***University of Cambridge Department of Chemical Engineering and Biotechnology, Philippa Fawcett Drive, Cambridge. CB3 0AS.***

## Abstract

A horizontal soap film is established in vertical tube a few centimetres in diameter. A metal sphere, 1-2mm diameter, is dropped onto the film, whose distortion is observed by means of a high speed camera. The film wraps partly around the sphere, detaching at a circle which moves up the sphere as it falls.

The shape of the film at successive radii, bigger than the radius of contact, was predicted from theory relying on the proposition that if both sides of the film are open to atmosphere, there can be no pressure difference across it. The pressure difference across a film is proportional to (surface tension) / (radius of curvature); hence it follows that the radii of curvature in two planes, perpendicular to each other and to the film surface, must be equal and opposite. This proposition gives equations predicting the shape, in reasonable agreement with experiment.

This theory is compared with the theory of catenoids, first studied by Euler in 1744. Catenoid theory gives exactly the same results as the 'radius of curvature' theory presented here. A simple energy conservation argument shows that the two theories are compatible and agree with a published photograph of a soap film catenoid.

**Keywords: foams, thin liquid films, froth flotation, bubbles, liquid menisci.**

**Subject areas: fluid mechanics, chemical engineering.**



**Draft date: 17th April 2019**

## 1. Introduction

A dry foam, *i.e.* a foam containing a small volume fraction of liquid, consists of (a) thin soap films joined to (b) menisci, each of which may connect several soap films. Here we are concerned with a single soap film and its behaviour when a small solid sphere is dropped through it. This is relevant to froth flotation, where a foam is used to separate the components of a mixture of solid particles, for example coal and stone; one component sinks and the other floats.

Here we consider what must be an important feature of froth flotation, namely how does a thin soap film distort when a small particle strikes it in a direction normal to the plane of the film? This was studied using a '*soap film meter'*. This is a vertical glass tube, typically a few centimetres diameter, whose internal wall is wetted with soap solution. This solution is introduced at the bottom and gets carried up as a thin horizontal film by a gas flow to be measured by timing the film transit between two marks on the tube wall. The transit time, together with the known volume between marks, gives an unequivocal measure of flow rate.

Here we use the soap film meter differently. A single film is introduced into the tube; then by controlling the air input at the bottom, this single film can be positioned opposite a camera to detect its distortion. The distortion is due to a small metal sphere, 1 or 2 mm diameter, dropped a few millimetres onto the film. The film wraps round the sphere; the observed distortions are compared with theoretical analysis. The basis of this analysis is to postulate that there is no pressure difference across the film, both sides being open to atmosphere.

This assumption of zero pressure drop leads to the conclusion that the radius of curvature, $R_1$, of the film in one direction is equal and opposite to $R_2$, the radius of curvature in a plane perpendicular to that of $R_1$. The pressure difference across the film, $\Delta P$, depends on surface tension, $\sigma$, and these radii of curvature and is given by the Young-Laplace law[1] *viz*

$$\Delta P = \sigma\left(\frac{1}{R_1}+\frac{1}{R_2}\right) = 0 \qquad \textbf{(1)}$$

This leads to the conclusion that $R_1 = -R_2$, and subsequently gives a formula to predict the film shape. This formula can then be compared with shapes observed by photography.

This work has much in common with the study of catenoids, which dates back to the time of Euler (Euler, 1744; Oldfather et al., 1933; Orr et al., 1975). Here, the criterion determining the shape is that of minimal area between constraints, which is shown to be identical with the above criterion, *i.e.* $R_1 = R_2$. This criterion is also discussed by Plateau in the context of defining minimal surfaces (Plateau, 1873)[2].

## 2. Literature survey

There are many publications on foams and related topics. Here, we refer only to publications relevant to the prime subject of this paper, namely the behaviour of a thin horizontal soap film when a small sphere (or perhaps droplet) falls onto it. We also allude briefly to the substantial literature on minimal surfaces and catenoids, whose study dates back to Euler in 1744.

### *2.1. Sphere falling through a horizontal soap film: geometry*

[1] The fascinating history underlying the derivation of this relationship is given in a paper by Craik (Craik, 2010).
[2] An English translation of this work has been made available by Kenneth A. Brakke at http://facstaff.susqu.edu/brakke/aux/downloads/Plateau-Eng.pdf

The paper most relevant to our work is that of Le Goff and co-workers (Le Goff et al., 2008). Their primary concern was the behaviour of a sphere passing through a '*bamboo foam'*, *i.e.* a series of horizontal soap films, one above the other; but they give a sequence of photographs showing a 3.2 mm diameter sphere passing through a horizontal soap film. These photographs show the film wrapping around the sphere and eventually detaching, whereupon the film healed.

Also of direct relevance is the works of Davies (Davies and Cox, 2012; Davies, 2018) where numerical simulations are presented that describe the distortion of a horizontal soap film when a spherical and '*super quadric*' object falls through it. The falling object was either spherical bead or roughly a cube with rounded corners and edges. A finite contact angle between the film and the cube was assumed. This work was the inspiration for the present study. The interaction between super quadric objects and soap films has also been studied extensively by Morris (Morris et al., 2012, 2010) and is of relevance to the separation of cubic crystals of lead ore (galena) from mining tailings using froth flotation (Morris and Cilliers, 2014). A review of the subject by the same author (Morris et al., 2015) gives a good summary of the energetically stable orientations of both spherical and cubic particles captured on the surface of a soap film.

Note that the work of Le Goff and co-workers (Le Goff et al., 2008) was entirely experimental and involved fast-moving objects, whereas that of Davies (Davies, 2018) and Morris and co-workers (Morris et al., 2012, 2010) was theoretical and quasi-static. Here we compare theory with experiment for the simplest case, that of a sphere falling vertically through a horizontal soap film.

### *2.2. Interaction between a falling sphere and a soap film: dynamics*

Whereas our work is concerned entirely with the geometry of the soap film as it wraps around the falling sphere, many authors have studied the dynamics to answer such questions as (i) will the sphere fall right through the film? (ii) will the sphere be held on the film? (iii) will the sphere bounce back after striking the film? For example, one study (Courbin and Stone, 2006) observed the motion of a liquid droplet striking a film which it did not puncture; the film was observed to recover its original shape, post impact. Other studies (Albijanic et al., 2014; Stechemesser and Nguyen, 1999; Verrelli et al., 2011) have determined whether a particle will attach to a film. When a particle passes through a film some of the film liquid may remain attached to the top side of the sphere after penetration. One study (Gilet and Bush, 2009) developed a criterion to predict the boundary between (i) a droplet bouncing on a soap film and (ii) the same droplet passing through the film. Kim and Wu (2010) studied the impact of very small droplets, diameter about 25 μm, with a thin vertical soap film to characterize the energy required to tunnel through the soap film. One study (Kirstetter et al, 2012) demonstrated the existence of three different flow scenarios resulting from the impact of a liquid jet onto a thin soap film: refraction, absorption and reflection regimes. Recent research by Stogin and co-workers (Stogin et al., 2018) reports the use of liquid membranes to act as a size-exclusion separation device: large particles pass through the liquid film whereas small particles are captured, demonstrating some potential practical applications such as (i) insect and particle barriers, (ii) self-cleaning, non-fouling membranes for continuous particle separation, (iii) surgical films, and (iv) gas/odour barriers.

Numerical simulations (Davies and Cox, 2012) have shown the importance of the Bond number, $Bo = \frac{\rho g d^2}{4\sigma}$, in determining the motion of a sphere passing through a succession of horizontal soap films, a '*bamboo foam*'. Here, $\rho$ is the solid density, $g$ the acceleration due to gravity, $d$ the particle diameter and $\sigma$ the air-liquid surface tension.

### *2.3. Minimal surfaces and catenoids*

A catenoid can been defined as '*…a type of surface, arising by rotating a catenary curve about an axis'* (Dierkes et al., 2010). Furthermore, a catenoid can be described as being '*…a minimal surface,*

*meaning that it occupies the least area when bounded by a closed space'* (Gullberg, 1997). Catenoids were first described by Leonard Euler in 1744 in his work '*Methodus inveniendi lineas curvas maximi minimive proprietate gaudentes, sive solution problematis isoperimetrici latissimo sensu accepti accepti (A method for finding curved lines enjoying properties of maximum or minimum, or solution of isoperimetric problems in the broadest accepted sense)*' (Euler, 1744). This work has been faithfully translated (Oldfather et al., 1933) from the Latin and gives a fascinating insight into the first research into these highly relevant shapes: it emerges, as shown below, that the film shapes generated when a sphere falls through a soap film are catenoids.

Every soap film is a physical model of a minimal surface, as the surface tension tries to shrink the surface as much as possible; catenoids belong to the family of minimal surfaces: a minimal surface can be defined to be one where the mean curvature vanishes identically (Oprea, 2000; Pérez, 2017). Other examples of minimal surfaces include helicoids (Colding and Minicozzi, 2006) and gyroids (Schoen, 1970). The minimal surface formed when a soap film bridges two rings of equal radii is a symmetric catenoid (Seiwert et al., 2013; Salkin et al., 2014). An asymmetric catenoid is formed when a soap film is withdrawn from a bath of surfactant solution by a ring (Salkin et al., 2014). An asymmetric catenoid also forms when a symmetric catenoid collapses onto a cylindrical rod held on its axis of symmetry (Moffatt et al., 2016). The dynamics of a collapsing catenoid, analogous to those of a rupturing soap film, has been investigated computationally (Chopp and Sethian, 1993) and experimentally (Ito and Sato, 2010; Robinson and Steen, 2001), giving insight into the conditions required for film stability. With two rings of unequal radii, two different portions of catenoid are formed, connected by a flat soap film, resulting in more complex stability problem.

## 3. Theory: a sphere falling onto a horizontal soap film.

Figure 1 shows a solid sphere of diameter $d$ falling onto a soap film. The film is assumed to wrap around the bottom of the sphere and then to detach from the sphere at angle $\psi$, with zero contact angle: thus, the film is tangent to the sphere at the point of contact. This assumption stems from experimentally-observed film shapes that are discussed in Section 5 and illustrated in Figure 8.

<FIGURE 1>

Upon leaving the point of contact with the sphere, the film forms a shape determined by the assumption that there is zero pressure difference across the film; this follows from the fact that, at a big horizontal radius from the vertical axis, the film must asymptote to be nearly horizontal. Also, it was observed during the experiments that the outer region of the film near the meniscus did not move, implying zero pressure difference across the film. This fact of zero pressure drop implies that the radius of curvature in the plane of observation, $R_1$, must be equal and opposite to $R_2$, the radius of curvature in the plane normal to the plane of observation. This follows from the fact that the pressure difference, $\Delta P$, across a film is

$$\Delta P = \frac{2\sigma}{R} \qquad \textbf{(2)}$$

Here, $\sigma$ is the surface tension, $R$ the radius of curvature and the factor 2 is included since the film is double-sided. Note that the above, and its development below, is quasi-static: the mass-acceleration of the film is ignored. Bearing in mind that the soap film is a few micrometres thick, its inertia effect must be negligible in comparison with the surface tension forces.

Figure 1 shows the geometry arising from the above. The radius of curvature in the plane of the diagram, $R_1$, is given by the well-known expression

$$R_1 = -\frac{\left[1 + \left(\frac{dz}{dr}\right)^2\right]^{\frac{3}{2}}}{\frac{d^2z}{dr^2}}$$

**(3)**

Here, $(r, z)$ are cylindrical co-ordinates with their origin at the centre of the sphere (as shown in Figure 1). The radius of curvature in the plane normal to the diagram, $R_2$, is also shown in Figure 1. It is the distance, along a line normal to the film, between the film surface and the vertical axis through the centre of the sphere. Figure 1 shows how this arises: the upper right-hand part of the diagram shows a view, looking along arrow V, of the film as seen in a plane normal to the paper. Points A, A′and B are on the film, and from the diagram on the upper right of Figure 1, the three points lie on a circle of radius $R_2$, which is the radius of curvature in a plane normal to that of the paper. From the geometry, at all points on the film,

$$R_2 \sin\phi = r$$

**(4)**

and

$$\tan\phi = \frac{dz}{dr}$$

**(5)**

Eliminating $\phi$ between Equations (4) and (5), putting $R_1 = R_2$ for zero pressure difference across the film gives, using the definition of $R_1$ from Equation (3),

$$-r = \frac{\left(\frac{dz}{dr}\right)\left[1 + \left(\frac{dz}{dr}\right)^2\right]}{\frac{d^2z}{dr^2}}$$

**(6)**

Making a substitution $u$, where $u = \frac{dz}{dr}$, allows Equation (6) to be written

$$\frac{du}{u(1+u^2)} = -\frac{dr}{r}$$

**(7)**

Using the boundary condition that the film is tangent to the sphere at the point of detachment, *i.e.* where the film loses contact with the sphere, $\frac{dz}{dr} = \tan\psi$ when $r = \frac{d}{2}\sin\psi$, This assumption, that the film is nearly tangent to the sphere at the point of detachment, is consistent with experimental observation: see, for example, Figure 6 or Figure 8. These photographs suggest an angle of contact in the range 0-30°. Equation (7) is readily integrated to give

$$\left[-\ln r\right]_{\frac{d}{2}\sin\psi}^{r} = \left[\ln u - \frac{1}{2}\ln(1+u^2)\right]_{\tan\psi}^{u}$$

**(8)**

Here, $\psi$ is the angle of contact of the film, see Figure 1. After some manipulation, Equation (8) gives:

$$u = \frac{dz}{dr} = \left[\left\{2\left(\frac{r}{d}\right)\csc^2\psi\right\}^2 - 1\right]^{-\frac{1}{2}} \tag{9}$$

This, in turn, may be integrated between the limits $r = \frac{d}{2}\sin\psi$ to $r$, giving:

$$\frac{z}{d} = \frac{\cosh^{-1}\left\{2\left(\frac{r}{d}\right)\csc^2\psi\right\} \pm \cosh^{-1}(\csc\psi)}{2\csc^2\psi} - \frac{\cos\psi}{2} \tag{10}$$

Equation (10) may be inverted to give $r$ in terms of $z$, which is more convenient because, as shown below, there are, for $90^\circ < \psi < 180^\circ$, two values of $z$ for $r < \left(\frac{d}{2}\right)\sin\psi$. From Equation (10) it follows that

$$\frac{2r}{d}\csc^2\psi = \cosh\left[\left(\frac{2z}{d} + \cos\psi\right)\csc^2\psi \mp \cosh^{-1}(\csc\psi)\right] \tag{11}$$

The minus sign in Equation (10) is for $0 < \psi < 90^\circ$, and the plus sign is for $90^\circ < \psi < 180^\circ$; but for $r < \left(\frac{d}{2}\right)\sin\psi$, both plus and minus are used in Equation (10) to give the two values of $z$ mentioned above. In Equation (11), the plus sign is for $0 < \psi < 90^\circ$; the minus sign is for $90^\circ < \psi < 180^\circ$. The above results, equations (10) and (11), are special cases of the more general theory given by Orr et al (1975).

### *3.1. Theoretical curves showing film shapes*

Figure 2 shows the film shapes from Equations (10) or (11) for a range of values of $\psi$. Notable features of the curves are as follows.

<FIGURE 2>

(i) *Radii of curvature*

When $\psi > 90^\circ$, the curves show $\frac{dz}{dr} \to \infty$ at the point of inflection. It is clear that, at this point, $R_1 = R_2$, e.g. for $\psi = 135^\circ$. Of course, at all points $R_1 = R_2$, but this is most evident for the cusps where $\psi > 90^\circ$.

(ii) *Asymptotes for large $r$*

From Figure 2 it appears that there is no asymptote for large radius, $r$. This arises from the first $\cosh^{-1}$ term in Equation (10), which has no asymptote: $\cosh^{-1} y$ increases progressively with $y$, albeit more slowly for large $y$. This is important when comparing theory and experiment, as discussed in Section 5.

(iii) *Sequence of curves for larger values of $\psi$, i.e. $90^\circ < \psi < 180^\circ$.*

<FIGURE 3>

Figure 3 shows the sequence of film shapes for large values of $\psi$. In this region of $\psi$, after contact the film radius at first reduces and then increases; thus for radii less than the radius of contact there are two values of $z$.

Another important feature of the curves is that, in the region $\frac{r}{d} > 1$ , the curves show that at a given $\frac{r}{d}$, $\frac{z}{d}$ at first increases with $\psi$ but then $\frac{z}{d}$ decreases, so that at $\psi = 170^{\circ}$, for example, the value of $\frac{z}{d}$ is much less than for smaller values of $\psi$ (see Figure 3). Thus when $\psi$ approaches $180^{\circ}$, the detaching film is almost flat and level with the top of the sphere. This variation of the film shape with $\psi$ is important in comparing theory with experiment.

(iv) *Film shape for* $\psi = 90^{\circ}$

The shape seen for $\psi = 90^{\circ}$ resembles an 'asymmetric catenoid', as would be observed with a soap film joining two rings, the smaller ring having the radius of the sphere in Figs 2 or 3.

## 4. Experimental

<FIGURE 4>

Figure 4 shows the equipment. The film was formed in the vertical tube, the '*soap film meter*', with diameter $D = 8.6$ mm. The soap film was generated by two alternative methods described in section 4.2. An air inlet, at the bottom, enabled the soap film to be moved up or down the tube; the film was placed level with the camera and light source. Once the film was in the desired location, the air inlet was left open to atmosphere, thus ensuring that there was no pressure difference across the film. This justifies the use of the zero pressure difference assumption in the theory described in Section 3.

A small spherical particle, chrome steel grade 100, diameter $d = 1.6$ mm or $d = 2.0$ mm, was held on the tip of the hypodermic needle, the end of which was squared off to enable the sphere to be held by suction provided by a syringe pump (World Precision Instruments). On releasing the suction, the sphere fell onto the film, whose motion (and that of the sphere) was photographed at 550 frames per second using a high speed camera (Basler acA640-750um).

### *4.1. Soap solutions*

The soap solution contained three components:

i. a surfactant consisting of Fairy Liquid (Proctor & Gamble);
ii. a stabiliser consisting of glycerol (99% assay);
iii. de-ionised water.

A number of compositions were tried; the prime difficulty was that film rupture occurred immediately the sphere contacted the film. After some trials, the chosen composition that provided a stable film was a volumetric ratio of (surfactant : glycerol : water) of 1:12:6. This was somewhat different to formulations used in other studies (Le Goff et al., 2008), where 1:12:2 was used. Fairy Liquid was chosen as the surfactant due to its benign nature and widespread availability should others wish to reproduce this work.

### *4.2. Formation of the soap film*

Two methods were employed to obtain a soap film positioned in the camera's plane of view.

i. *Generation from the bottom: 'bottom up'*

This follows the normal procedure when the tube is used as a meter for airflow measurement. The solution was put into the rubber holder at the bottom of the tube, see Figure 4. With airflow

introduced at the bottom, the rubber holder containing surfactant solution was squeezed to give a film, carried up by the airflow; this was stopped when the film was level with camera and light source.

With this method, the film travelled about 15 cm up the tube, often rupturing on the way. When the film did not rupture, air bubbles were often entrained into film and into the meniscus on the wall.

ii. *Generation from the top: 'top down'*

An alternative method of forming the film was as follows. The soap film meter tube was inverted and lowered into soap solution to form a film across the top of the tube. The film was then drawn down by sucking air out of the bottom of the tube. For reasons that are uncertain, this method gave a reliably more stable film that often healed after being punctured by the falling sphere. Thus it was possible to do up to three separate experiments using the same film.

iii. *Comparison of the two methods of film formation*

Although 'top down' film generation was easier than the 'bottom up' method, the latter did have certain advantages. As shown below, the 'bottom up' method gave a smaller meniscus, making it easier to obtain clear photographs of film deformation as the sphere fell through it. The meniscus generated using the 'top down' method was thicker, hence a significant portion of the film motion during deformation was obscured from view.

### *4.3. Procedure for observing the film deformation.*

As shown in Figure 4, the small sphere was held above the soap film by suction through a square-ended hypodermic needle. The drop height, $h$, was chosen to give a small impact velocity, $v$, to permit a significant number of images to be taken at 550 frames per second. For the experiments shown, $h = 3.52\ \text{mm} \pm 0.21\ \text{mm}$, giving an impact velocity $v = \sqrt{2gh} = 0.26 \pm 0.01\ \text{m/s}$.

Thus in 20 ms, a typical observation duration, there were about 10 or 11 frames that captured the film deformation. During this observation time, the sphere would fall about 5 mm, *i.e.* two or three sphere diameters.

## 5. Results and discussion

<FIGURE 5>

Figure 5 shows a photograph of the soap film with its meniscus before a sphere was dropped through the film. The primary feature is the meniscus on the tube wall, of shape shown in Figure 5b. The height of the meniscus, the dark band in Figure 5a, was about 1.4 mm. The thin light band, barely visible in Figure 5a, is the soap film. The film is more apparent in other photographs, for example that shown in Figure 8.

<FIGURE 6>

Figure 6 shows a 2 mm sphere entering soap films generated by the two alternative methods. Figure 6a shows a film generated by the 'top down' method (described in Section 4.2ii). Figure 6b shows a film generated by the 'bottom up' method (described in Section 4.2i). It is clear that the 'bottom up' method, though more difficult to operate, gives a smaller meniscus and a more visible thin film, as shown by the white line in Figure 6b. Note that in Figure 6b the form of the film is similar to the theoretical result, Figure 2, with $\psi = 45^{\circ}$.

<FIGURE 7>

Figure 7 shows the sequence of film shapes for a sphere falling right through a soap film. The film shapes are similar to those reported in other studies (Le Goff et al., 2008). Note the rapid movement of the contact point between 5.5 ms and 7.3 ms. This may be explained by the sequence of film shapes

shown in Figure 3. From these shapes, it appears that the film moves predominantly upwards for $90^\circ < \psi < 120^\circ$; for larger values of $\psi$, *i.e.* $130^\circ < \psi \leq 180^\circ$, the film moves downwards to $\psi = 180^\circ$ when it is horizontal and contacts the sphere at its top. At $\psi = 130^\circ$ it appears that the film is fully stretched, corresponding to maximum surface energy (Le Goff et al., 2008; Stogin et al., 2018). As $\psi > 130^\circ$, the area of the film shown in Figure 3 appears to decrease, with the film moving rapidly to $\psi = 180^\circ$, returning the film to its un-stretched state. This may give some insight into the rapid film motion culminating in detachment observed in Figure 7 between 5.5 ms and 7.3 ms.

<FIGURE 8>

Figure 8 shows the sequence of images for a sphere falling through a film that did not rupture: the film healed when the sphere passed through it. Again, the film shapes are strikingly similar to those presented in other studies (Le Goff et al., 2008).

<FIGURE 9>

Figure 9 shows a comparison between the observed film shape and the theoretical predictions from Equations (10) and (11). The agreement between theory and experiment is good but not perfect. Two reasons for the difference can be conjectured.

i. The theory assumes zero contact angle at contact, *i.e.* that the film is tangential to the sphere. The photograph in Figure 9 suggests that there may be a finite contact angle, perhaps between $10^\circ$ and $20^\circ$. Note that there are two contact angles, the film being double sided. Thus, for the theory of section 2 above, the assumption of zero contact angle for the whole film may be inappropriate, which may account, at least partly, for the differences between theory and experiment in Figure 9.

ii. The other source of disagreement between theory and experiment is the behaviour of the film at the tube wall. The curves in Figure 2 and Figure 3 imply that the theory does not predict a common asymptote: for large values of $r$, the film position, $i.e.$ the value of $z$ at large $r$, moves up and down according to the value of the contact angle, $\psi$. It is manifestly clear from the photographs in Figures 6 to 8 that the meniscus, and consequently the film, near the wall remains stationary. This may account, partly, for the differences between theory and experiment shown in Figure 9.

## 6. Catenoids

<FIGURE 10>

Work undertaken in another study (Cryer and Steen, 1992) examined the behaviour of a soap film between two co-axial rings: a photograph of a typical result in shown in Figure 10. This shape is that of a catenoid. Superimposed on this photograph is a sequence of dots, which were derived from Equations (10) and (11) with $\psi = 90^\circ$, corresponding to a film contact point positioned at the equator of the sphere in our work. There is remarkably good agreement between the theory and the photographed profile.

As noted in the introduction, the study of catenoids dates back as far as Euler (Euler, 1744; Oldfather et al., 1933). He, and successors, have used the fact that catenoids have minimal surface area. That is equivalent to the zero value of $\Delta P$, the pressure drop across the film, and can be proven as follows.

Suppose a film is established using the zero pressure drop criterion. Now impose a finite pressure drop, $\Delta P$, across the film, where $\Delta P$ may be positive or negative. Imposing finite $\Delta P$ implies an energy input to the film, and hence an increase in the film area because the energy stored is proportional to the product of the surface tension and the film area. Hence if surface area is plotted as a function of $\Delta P$, there must be a minimum when $\Delta P = 0$. This implies that minimising surface area

is equivalent to getting equal and opposite values of the radius of curvature, as described in Section 3. The equation for a simple catenoid can be written as (Taylor and Michael, 1973)

$$r = c\cosh\left(\frac{z}{c}\right) \tag{12}$$

Here, $c$ is a constant. Equation (12) is of exactly the same form as Equation (11) with $\psi = 90^{\circ}$, further proof that the criterion of equal and opposite radii of curvature at all points gives the same answer as minimising the surface area.

## 7. Conclusions

Experiments to observe the distortion of a horizontal soap film due to a sphere striking the film vertically are reported. The film shapes observed by high speed photography are in reasonably good agreement with theory. The theory is based on the fact that there must at all times be zero pressure difference across the film; it follows that the two radii of curvature, $R_1$ and $R_2$, in two perpendicular planes normal to the film, must be equal and opposite, *i.e.* $R_1 = -R_2$. This leads to equations that predict the shape of the film as it is deformed by the falling sphere.

Differences between theory and experiment may be due to two factors:

i. the theory assumes zero contact angle between film and sphere. The actual contact angle may be finite;
ii. the theory predicts that, at large horizontal distances from the axis of the sphere, the film is not flat *i.e.* it has a finite slope, albeit small.

This latter point implies that where the nearly horizontal film meets the wall of the vertical tube containing the film, the contact point should, according to theory, move up and down. Observations show that where the film meets the tube wall, in the form a meniscus, there is no movement. This may explain the differences, albeit small, between theory and experiment.

The work reported here is linked to work on catenoids, surfaces of minimum area, on which there are many publications. It is shown that the minimum surface area criterion gives the same answer as the above-mentioned proposition of equal and opposite radii of curvature.

## 8. Acknowledgements

The work was supported by EPSRC contract number EP/N00230X/1. The authors are grateful to P.J. Davidson, who initiated the project.

## 9. Attributions

**Data accessibility**. All datasets presented in this work would be available on request.

**Author's contributions.** The project was conceived by JFD, CHC and BH. The experimental work was done by CHC, AP and PJ. The theory was developed by JFD, CHC, AP and PJ. The text was written by JFD and BH. The literature survey was done by BH, AP and PJ.

**Competing interests.** The authors have no competing interests.

## Nomenclature

### Roman letters

| | | | |
|---|---|---|---|
| $c$ | - | Constant in catenoid equation | (m) |
| $D$ | - | Tube diameter | (m) |
| $d$ | - | Sphere diameter | (m) |
| $g$ | - | Acceleration due to gravity | (m/s$^2$) |
| $h$ | - | Height of sphere above soap film | (m) |
| $\Delta P$ | - | Pressure drop across soap film | (Pa) |
| $R$ | - | Radius of curvature | (m) |
| $R_1$ | - | Radius of curvature in plane of observation | (m) |
| $R_2$ | - | Radius of curvature perpendicular to $R_1$ | (m) |
| $r$ | - | Radial co-ordinate | (m) |
| $u$ | - | Substitution variable, $dz/dr$ | (-) |
| $v$ | - | Sphere velocity | (m/s) |
| $y$ | - | Variable | (m) |
| $z$ | - | Axial co-ordinate | (m) |

### Greek letters

| | | | |
|---|---|---|---|
| $\rho$ | - | Solid density | (kg/m$^3$) |
| $\boldsymbol{\sigma}$ | - | Surface tension | (N/m) |
| $\phi$ | - | Angle between vertical and point B, Figure 1 | (°) |
| $\psi$ | - | Film contact angle | (°) |

### Non-dimensional groups

| | | | |
|---|---|---|---|
| $\boldsymbol{Bo}$ | - | Bond number, $\boldsymbol{\rho g d^2/4\sigma}$ | (-) |

## List of figures

## References


Albijanic, B., Ozdemir, O., Hampton, M.A., Nguyen, P.T., Nguyen, A.V., Bradshaw, D., 2014. Fundamental aspects of bubble–particle attachment mechanism in flotation separation. *Miner. Eng.* 65, 187–195.

Chopp, D.L., Sethian, J.A., 1993. Flow under curvature: singularity formation, minimal surfaces, and geodesics. *Exp. Math.* 2, 235–255.

Colding, T.H., Minicozzi, W.P., 2006. Shapes of embedded minimal surfaces. *Proc. Natl. Acad. Sci. U. S. A.* 103, 11106–11.

Courbin, L., Stone, H.A., 2006. Impact, puncturing, and the self-healing of soap films. *Phys. Fluids* 18, 091105.

Craik, A.D.D., 2010. Thomas Young on fluid mechanics. *J Eng Math* 67, 95–113.

Cryer, S.A., Steen, P.H., 1992. Collapse of the soap-film bridge: quasistatic description. *J. Colloid Interface Sci.* 154, 276–288.

Davies, I.T., 2018. Simulating the interaction between a descending super-quadric solid object and a soap film. *Proc. R. Soc. A Math. Phys. Eng. Sci.* 474, 20180533.

Davies, I.T., Cox, S.J., 2012. Sphere motion in ordered three-dimensional foams. *J. Rheol.* 56, 473–483.

Dierkes, U., Hildebrandt, S., Sauvigny, F., 2010. Minimal surfaces. Springer.

Euler, L., 1744. De curvis elasticis, Methodus inveniendi lineas curvas maximi minimive proprietate guadentes, sive solutio problematis isoperimetrici latissimo sensu accepti. Marcum-Michaelem Bousquet & Socios, Lausanne and Geneva.

Gilet, T., Bush, J.W.M., 2009. The fluid trampoline: droplets bouncing on a soap film. *J. Fluid Mech.* 625, 167.

Gullberg, J., 1997. Mathematics : from the birth of numbers. W.W. Norton.

Ito, M., Sato, T., 2010. In situ observation of a soap-film catenoid-a simple educational physics experiment Related content In situ observation of a soap-film catenoid-a simple educational physics experiment. *Eur. J. Phys.* 31, 357–365.

Kim I., Wu X. L., 2010 Tunneling of micron-sized droplets through soap films. Phys. Rev. E 82, 026313

Kirstetter G., Raufaste C., Celestini F., 2012. Jet impact on a soap film. Phys. Rev. E 86, 036303

Le Goff, A., Courbin, L., Stone, H.A., Quéré, D., 2008. Energy absorption in a bamboo foam. *Europhys. Lett.* 84, 36001.

Moffatt, H.K., Goldstein, R.E., Pesci, A.I., 2016. Soap-film dynamics and topological transitions under continuous deformation. *Invit. Artic. Phys. Rev. Fluids* 1, 60503.

Morris, G., Hadler, K., Cilliers, J., 2015. Particles in thin liquid films and at interfaces. *Curr. Opin. Colloid Interface Sci.* 20, 98–104.

Morris, G., Neethling, S.J., Cilliers, J.J., 2012. Modelling the self orientation of particles in a film. *Miner. Eng.* 33, 87–92.

Morris, G., Neethling, S.J., Cilliers, J.J., 2010. The effects of hydrophobicity and orientation of cubic particles on the stability of thin films.

Morris, G.D.M., Cilliers, J.J., 2014. Behaviour of a galena particle in a thin film, revisiting dippenaar.

*Int. J. Miner. Process.* 131, 1–6.

Oldfather, W.A., Ellis, C.A., Brown, D.M., 1933. Leonhard Euler's elastic curves. *Isis* 20, 72–160.

Oprea, J., 2000. The mathematics of soap films : explorations with Maple. American Mathematical Society.

Orr, F.M., Scriven, L.E., Rivas A.P., 1975. Pendular rings between solids: meniscus properties and capillary force, J. Fluid Mech. Vol 67 pp. 723-742.

Pérez, J., 2017. A new golden age of minimal surfaces. *Not. AMS* 64, 347–358.

Plateau, J., 1873. Experimental and theoretical statics of liquids subject to molecular forces Only. Gauthier-Villars, Paris.

Salkin, L., Schmit, A., Panizza, P., Courbin, L., 2014. Influence of buoundary conditions on the existence and stability of minimal surfaces of revolution made of soap films. Am. J. Phys. 82, 839.

Robinson, N.D., Steen, P.H., 2001. Observations of singularity formation during the capillary collapse and bubble pinch-off of a soap film bridge. *J. Colloid Interface Sci.* 241, 448–458.

Schoen, H.A., 1970. Infinite periodic minimal surfaces without self-intersections. *NASA Tech. Rep. NASA-TN-D-5541*.

Seiwert, J., Monloubou, M., Dollet, B., Cantat, I., 2013. Extension of a suspended soap film: a homogeneous dilatation followed by new film extraction. *Phys. Rev. Lett.* 111, 094501.

Stechemesser, H., Nguyen, A. V., 1999. Time of gas–solid–liquid three-phase contact expansion in flotation. *Int. J. Miner. Process.* 56, 117–132.

Stogin, B.B., Gockowski, L., Feldstein, H., Claure, H., Wang, J., Wong, T.-S., 2018. Free-standing liquid membranes as unusual particle separators. *Sci. Adv.* 4, eaat3276.

Taylor, G.I., Michael, D.H., 1973. On making holes in a sheet of fluid. *J. Fluid Mech.* 58, 625.

Verrelli, D.I., Koh, P.T.L., Nguyen, A. V., 2011. Particle–bubble interaction and attachment in flotation. *Chem. Eng. Sci.* 66, 5910–5921.

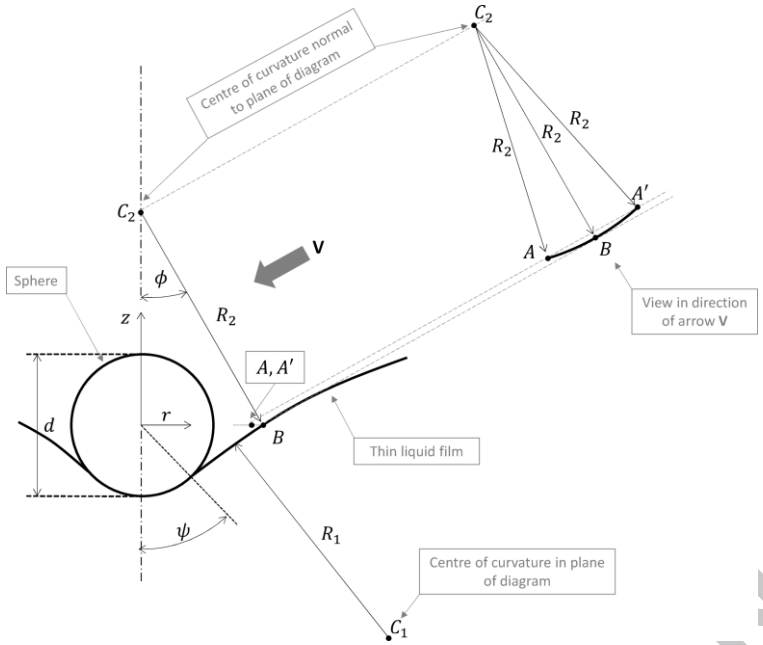
Centre of curvature normal to plane of diagram
$C_2$
$R_2$
$R_2$
$R_2$
$A'$
$A$
$B$
V
Sphere
$\phi$
$z$
$R_2$
View in direction of arrow V
$A, A'$
$d$
$r$
$B$
Thin liquid film
$\psi$
$R_1$
Centre of curvature in plane of diagram
$C_1$

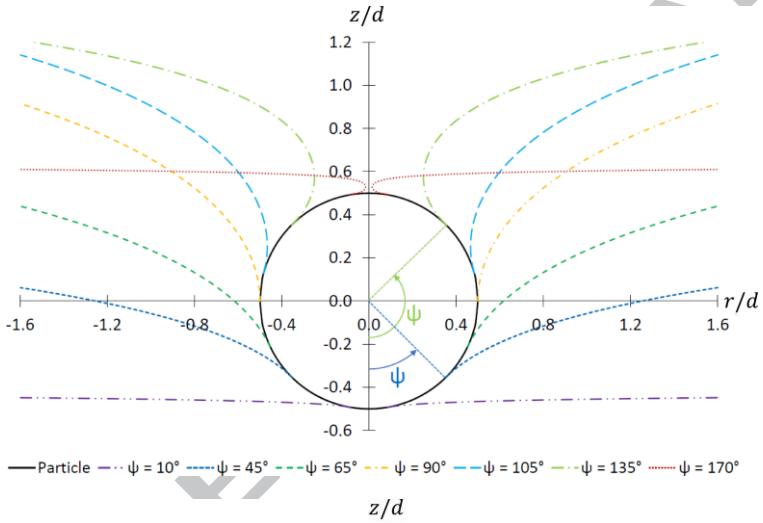
$z/d$
1.2
1.0
0.8
0.6
0.4
0.2
0.0
-0.2
-0.4
-0.6
-1.6
-1.2
-0.8
-0.4
0.0
0.4
0.8
1.2
1.6
$r/d$
ψ
ψ
Particle
ψ = 10°
ψ = 45°
ψ = 65°
ψ = 90°
ψ = 105°
ψ = 135°
ψ = 170°

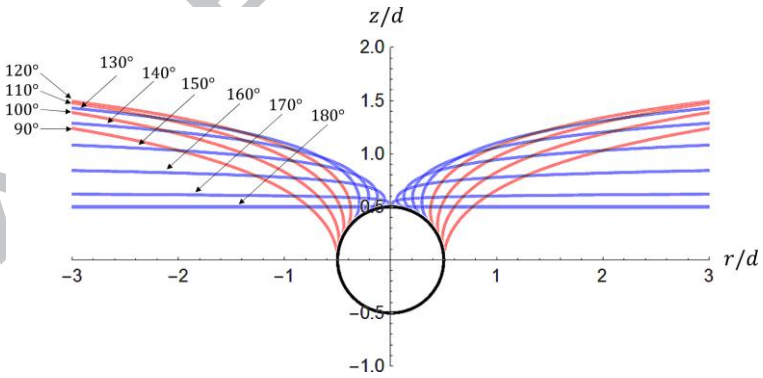
$z/d$
120°
110°
100°
90°
130°
140°
150°
160°
170°
180°
2.0
1.5
1.0
0.5
−0.5
−1.0
−3
−2
−1
1
2
3
$r/d$

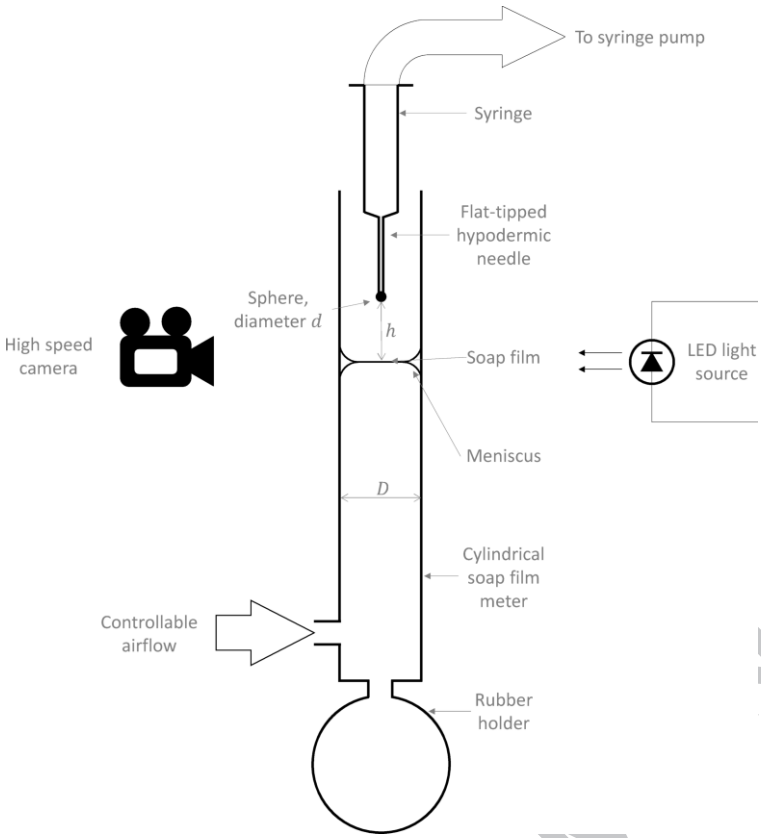
To syringe pump
Syringe
Flat-tipped hypodermic needle
Sphere, diameter $d$
High speed camera
$h$
Soap film
LED light source
Meniscus
$D$
Cylindrical soap film meter
Controllable airflow
Rubber holder

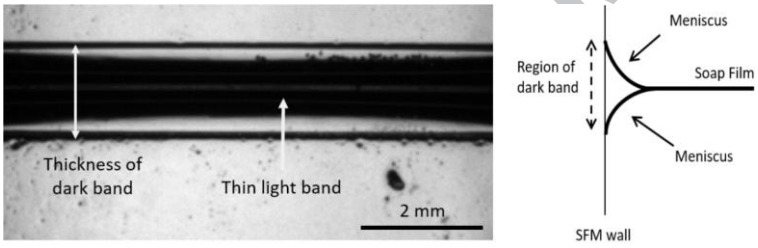
Thickness of dark band
Thin light band
2 mm
Meniscus
Region of dark band
Soap Film
Meniscus
SFM wall

(a) (b)


1 mm

(a) (b)

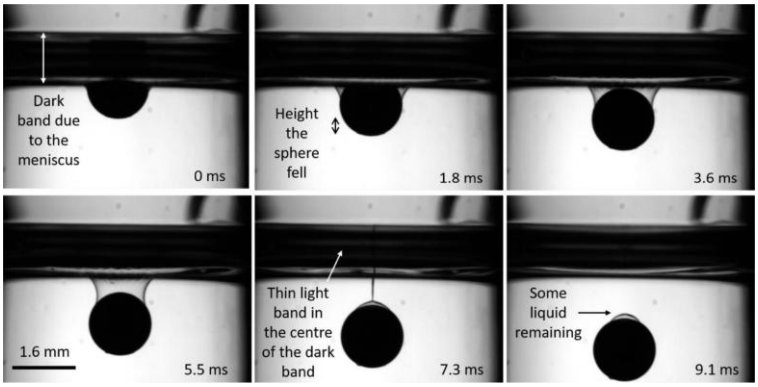
Dark band due to the meniscus
0 ms
Height the sphere fell
1.8 ms
3.6 ms
1.6 mm
5.5 ms
Thin light band in the centre of the dark band
7.3 ms
Some liquid remaining
9.1 ms

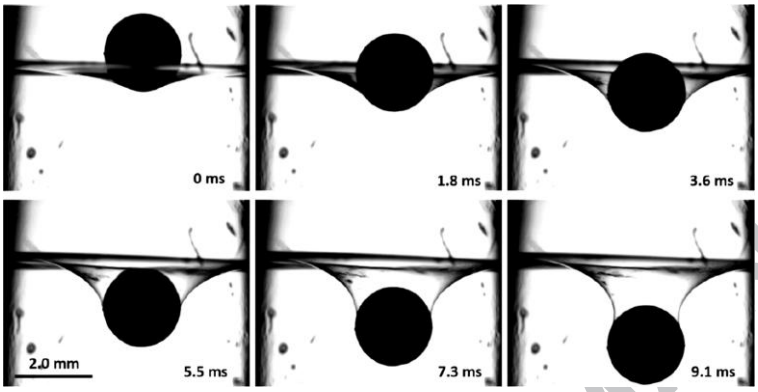
0 ms
1.8 ms
3.6 ms
2.0 mm
5.5 ms
7.3 ms
9.1 ms

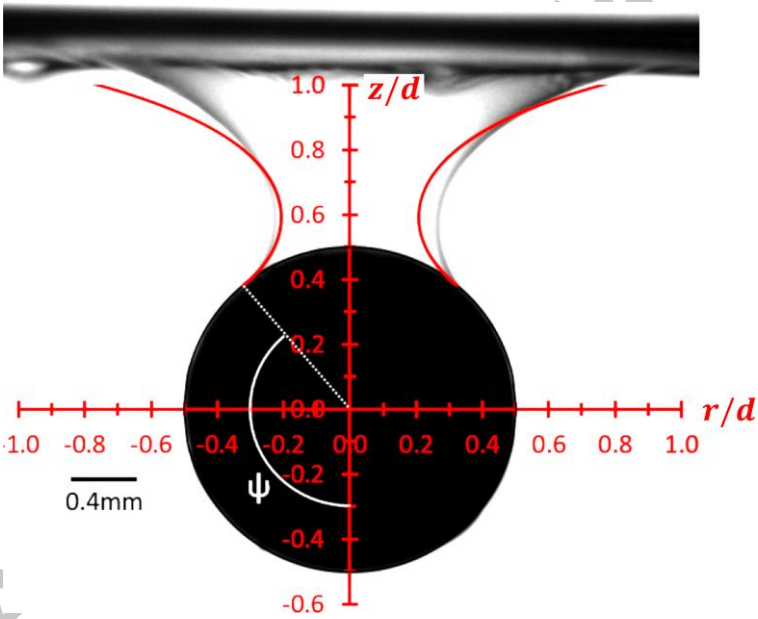
z/d
r/d
1.0
0.8
0.6
0.4
0.2
0.0
-0.2
-0.4
-0.6
-1.0
-0.8
-0.6
-0.4
-0.2
0.0
0.2
0.4
0.6
0.8
1.0
ψ
0.4mm

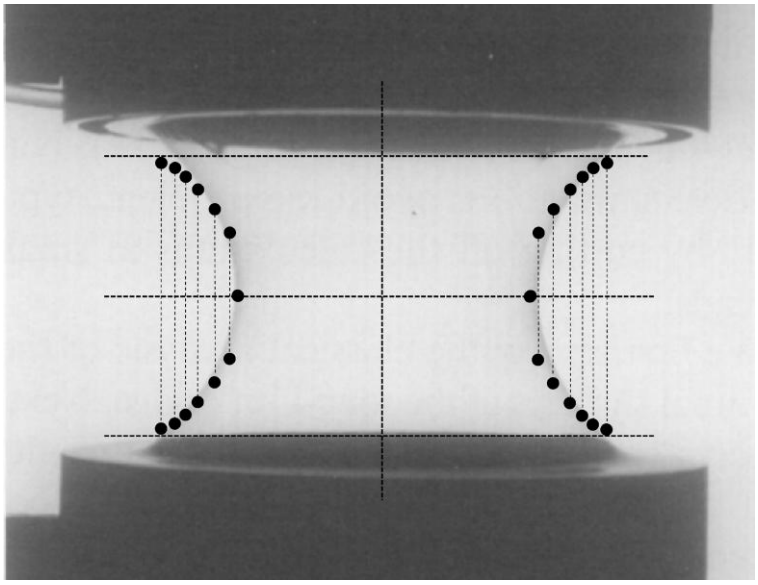

Graphical abstract

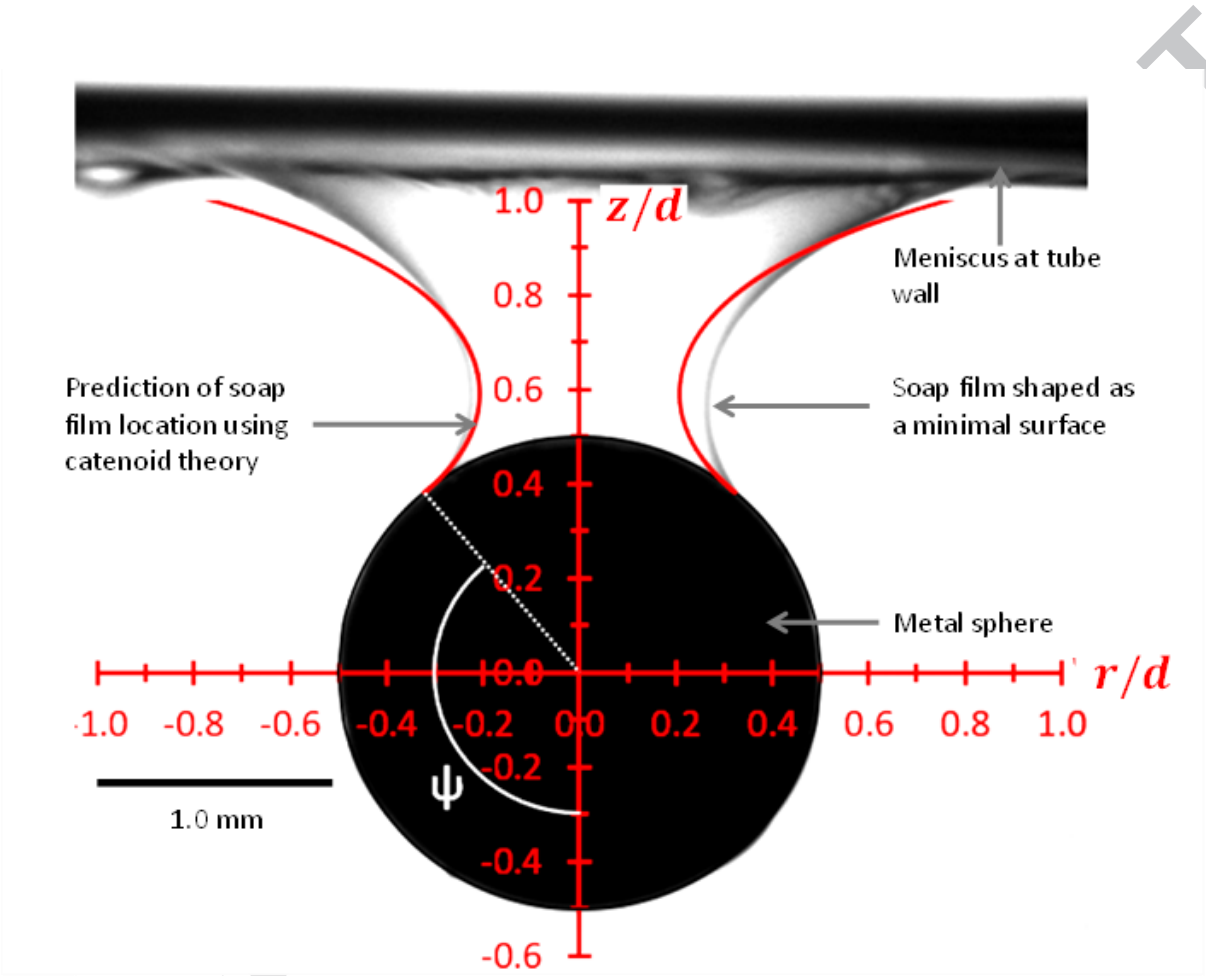

# The distortion of a horizontal soap film due to the impact of a falling sphere

**C.H. Chen, A. Perera, P. Jackson, B. Hallmark, J.F. Davidson**

***University of Cambridge Department of Chemical Engineering and Biotechnology, Philippa Fawcett Drive, Cambridge. CB3 0AS.***

## Highlights

- A small sphere, 1-2 mm diameter, falls through a horizontal soap film contained in a vertical tube 8.6 mm diameter. The soap film wraps round the sphere, detaching at angle $\psi$ as shown in the 'Graphical Abstract'.
- The sphere may bounce, or pass through the film before rupturing it.
- There is film rupture when the angle of detachment, $\psi$, is about $150^{\circ}$.
- Theoretical predication of film shape uses the assumption that $R_1 = R_2$, where $R_1$ is the radius of curvature in the plane of the diagram and $R_2$ is the radius of curvature normal to the plane of the diagram. $R_1 = R_2$ arises because there is no pressure difference across the film, the film being open to atmosphere on both sides.
- The condition $R_1 = R_2$ is equivalent to the postulate that the film surface area is minimal. This proposition has been used since 1744 (Euler) to predict the shape of a catenoid, for example, the film joining two concentric axial rings supporting a soap film between them.